Dapagliflozin activates AMPK to attenuate cardiac dysfunction and oxidative stress under hypoxia/reoxygenation-caused damage

Kun-Ling Tsai
National Cheng Kung University Hospital
Pei-Ling Hsieh
China Medical University
Wan-Ching Chou
National Cheng Kung University Hospital
Hui-Ching Cheng
National Cheng Kung University Hospital
Yu-Ting Huang
National Cheng Kung University Hospital
Shih-Hung Chan (chansh@mail.ncku.edu.tw)
National Cheng Kung University Hospital https://orcid.org/0000-0002-9064-1375

Original investigation

Keywords: Dapagliflozin, Ischemia/reperfusion injury, AMPK, Oxidative stress, Apoptosis

Posted Date: August 19th, 2020

DOI: https://doi.org/10.21203/rs.3.rs-51773/v1

Abstract

Background: Emerging evidence demonstrated Dapagliflozin (DAPA), an inhibitor of type II sodium-glucose cotransporter-2, prevented various cardiovascular events. However, the detailed mechanisms underlying its cardioprotective properties remained largely unknown. In the present study, we sought to investigate the effects of DAPA on the cardiac ischemia/reperfusion (I/R) injury and study the mechanisms of DAPA-provided cardioprotection.

Methods: For *in intro* studies, cardiac myoblast H9c2 cells were exposed to hypoxia with no-glucose medium for 1 hr than followed a reoxygenation with high-glucose medium for 4 hr. DAPA was treated before hypoxia/reoxygenation (H/R) exposure. For in vivo investigations, I/R was instigated in Sprague-Dawley (SD) rats using ligation of the left anterior descending coronary artery (LAD). DAPA was given daily by gavage for 5 days before I/R induction.

Results: Results from *in vitro* experiments showed that DAPA induced the phosphorylation of adenosine 5'-monophosphate activated protein kinase (AMPK), resulting in the downregulation of phosphorylated protein kinase C (PKC) in the cardiac myoblast H9c2 cells following H/R condition. We demonstrated that DAPA treatment diminished the H/R-elicited oxidative stress via the AMPK/ PKC/ NADPH oxidase (Nox) pathway. In addition, DAPA prevented the H/R-induced abnormality of peroxisome proliferator-activated receptor-gamma coactivator 1-alpha (PGC-1α) expression, mitochondrial membrane potential, and mitochondrial DNA copy number through AMPK/ PKC/ Nox signaling. Besides, DAPA reversed the apoptosis-associated changes, including H/R-suppressed Bcl-2 and H/R-induced expression of phosphorylated p53, Bax cytochrome c, and activated caspase 3 via AMPK/ PKC/ Nox/ PGC-1α signaling. Furthermore, we demonstrated that DAPA improved the I/R-induced cardiac dysfunction by echocardiography and abrogated the I/R-elicited apoptotic cells by terminal deoxynucleotidyl transferase dUTP nick end labeling assay in the myocardium of rats. Also, the administration of DAPA mitigated the production of two myocardial infarction markers, creatine phosphokinase isoenzymes and lactate dehydrogenase.

Conclusion: In conclusion, our data suggested that DAPA treatment holds the potential to ameliorate the I/R-elicited oxidative stress and the following cardiac apoptosis via AMPK/ PKC/ Nox/ PGC-1α signaling, which attenuates the cardiac dysfunction caused by I/R injury.

Introduction

In spite of the advances made in diagnostic and therapeutic approaches, the death rates and complications attributable to cardiovascular diseases (CVD) remained disturbingly high [1]. It has been shown that the long-term prognosis of patients with acute myocardial infarction (AMI) was not benign, especially when their left ventricular ejection fraction was ≤ 45% [2]. Hence, a vast amount of research effort has been devoted to the studies on myocardium salvage and reduction of infarction size. To date, the standard treatments of AMI are reperfusion strategies using either thrombolytic therapy or primary

percutaneous coronary intervention for maintaining the patency of the infarct-related coronary artery [3]. However, these approaches may inevitably result in undesirable ischemia/reperfusion (I/R) injury.

During the ischemia phase, the metabolism of the affected cells was altered and their energy-dependent function was impaired due to the reduced adenosine triphosphate (ATP) availability, which eventually leading to calcium overload, structural disorganization, and cell death. Later, the restoration of blood flow further exacerbated tissue damage as the unremitting generation of reactive oxygen species (ROS) aggravated cell death [4]. Mitochondrial ROS production has been shown to regulate redox signal and sensed by various enzymes, and one of them was adenosine 5'-monophosphate activated protein kinase (AMPK) [5]. It has been demonstrated that AMPK activation triggered a peroxisome proliferator-activated receptor gamma coactivator 1-alpha (PGC-1α)-dependent antioxidant response and the interplay between AMPK and PGC-1α participated in the control of ROS homeostasis [5]. Besides, results from studies using transgenic mice with impaired cardiac AMPK activation [6] or direct activation of AMPK by a small molecule [7] both supported that AMPK possessed the properties to regulate myocardial metabolism, and limit the apoptosis and cardiac dysfunction following I/R injury.

Dapagliflozin (DAPA) is a selective sodium-glucose transporter 2 (SGLT2) inhibitor, which can be used to reduce plasma glucose as it blocks glucose resorption in the kidney and induces glycosuria for patients with type 2 diabetes mellitus (DM) [8]. Recently, robust data from multiple clinical trials revealed the cardioprotective effects of DAPA. For instance, DAPA has been shown to be implicated in the improvement of myocardial function and reduced all-cause mortality in DM patients with chronic heart failure [9, 10]. Moreover, DAPA treatment led to a lower rate of cardiovascular death or hospitalization for DM patients who were at risk for atherosclerotic CVD [11] or had previous myocardial infarction [12]. Nevertheless, the molecular mechanism underlying its function in the heart has not been elucidated. Given that SGLT2 was mainly expressed in the kidney [13] and absent in the heart [14], it seemed SGLT2 may be excluded as a potential explanation for the direct cardioprotective effects of DAPA. In fact, one of the recent studies has revealed that DAPA induced anti-inflammatory responses in cardiofibroblasts stimulated with lipopolysaccharides through AMPK activation without the involvement of selective sodium-glucose transporters [14]. As such, we sought to examine whether DAPA exerted its beneficial effects on the heart subjected to I/R injury via AMPK and investigated the associated mechanisms.

To this end, we utilized cardiac myoblast H9c2 cells and assessed the AMPK phosphorylation in response to hypoxia/reoxygenation (H/R) condition. Subsequently, we dissected its signaling pathway and demonstrated how DAPA limited ROS production and apoptosis. Additionally, we verified that DAPA mitigated the cardiac damage caused by I/R injury and preserved the cardiac function *in vivo*.

Materials And Methods

Cell culture and reagents

H9c2 cells, which are myoblasts cells from rat myocardium, were purchased from the American Type Culture Collection. H9c2 cells were cultured with Dulbecco's modified Eagle's medium (DMEM)

supplemented with 10% fetal bovine serum (FBS) and penicillin (50 IU/mL)/streptomycin (50 µg/mL). A 0.25% (w/v) Trypsin-0.53 mM ethylenediaminetetraacetic acid (EDTA) solution was used to passage cells. Cells were cultured in humidified air with 5% CO^2 at 37°C. FBS and EDTA were purchased from Gibco (NY, USA). The 5,58,6,68-tetraethylbenzimidazolcarbocyanine iodide (JC-1), Ro-32-0432, and diphenyleneiodonium chloride (DPI) were purchased from Sigma (MO, USA). Dihydroethidium (DHE) was obtained from Thermo Scientific (MA, USA). Anti-β-actin, anti-phospho-AMPK, anti-AMPK, anti-Nox-2, anti-Rac-1, anti-phospho-PKC, anti-PKC, anti-phospho-p53, anti-Bax, anti-Bcl2, anti-cytochrome c, anti-Na/K ATPase, and anti-PGC-1a were all obtained from Santa Cruz Biotechnology (Santa Cruz, CA, USA). Horseradish peroxidase (HRP)-conjugated anti-rabbit and anti-mouse secondary antibodies were purchased from Transduction Laboratories (CA, USA).

Hypoxia and ischemia induction

H9c2 cells were washed two times with PBS to remove glucose and serum in the culture medium. In control cells, the medium was replaced with glucose-free DMEM; in DAPA-treated cells, the medium was replaced with DAPA containing glucose-free DMEM. The cells were transferred to a hypoxia chamber containing of 95% N2 and 5% CO^2 for 1 hr. After hypoxia exposure, the cells were placed in a 5% CO^2 and 95% O^2 incubator for reoxygenation with high-glucose DMEM containing of 10% FBS; in DAPA treated cells, DAPA was added to high-glucose DMEM. In animal study, vehicle or DAPA (0.1 mg/kg per day) was administered by the oral route. DAPA was dissolved in 60% propylene glycol and was given daily by gavage for 5 days before and 4 days after operation till sacrifice. For ischemia induction in animals, the heart was accessed by left thoracotomy, and the pericardium was removed in Sprague Dawley (SD) rats. Ischemia was induced via the ligation of the left anterior descending coronary artery (LAD) with a 6-0 silk suture. After 1 hr, ligation of LAD was released to allow reperfusion. The animals in the control group underwent the same surgical procedures but without LAD ligation. Four days after surgery, the animals were sacrificed for further experiments.

Protein isolation, tissue extraction and Western blotting assay

Protein expression levels were investigated by Western blotting. Total protein was isolated from cells of the left ventricle. After sacrifice, the hearts of all the animals were collected. The tissue of left ventricle was washed 2 times with PBS buffer, and then 100 mg of tissue was cut for homogenization with radioimmunoprecipitation assay (RIPA) lysis buffer. The homogenates were centrifuged at 13,000×g for 30 min, and the supernatant was collected and placed at −80 °C until use. The proteins were transferred to a polyvinylidene difluoride (PVDF) membrane after the proteins were separated by electrophoresis on sodium dodecyl sulfate polyacrylamide gels. The membranes were blocked by buffer for 1 hr at 37 °C. Then, the membranes were incubated with primary antibodies for 18 hr at 4 °C followed by hybridization with HRP-conjugated secondary antibodies for 1 hr. The intensities were quantified by densitometric analysis. Plasma was obtained through blood collection for lactate dehydrogenase (LDH) and creatine kinase-MB (CK-MB) assay.

Determination of cardiac functional parameters

Four days after operation, echocardiography was performed to assess cardiac function. Isoflurane-anesthetized animals were placed in a supine position. Echocardiographic data were collected by a Vevo 770 microimaging system with a 25-MHz probe (VisualSonics, Toronto, ON, Canada). Parameters were collected based on the M-mode and two-dimensional images obtained in the parasternal long and short axes at the level of the papillary muscles.

Apoptotic assay

Apoptotic cells were analyzed by the ApopTag® Peroxidase In Situ Apoptosis Detection Kit (Calbiochem). After H/R treatment, cells were rinsed twice in PBS before fixation for 30 min at room temperature with 4% paraformaldehyde. Next, cells were washed in PBS before incubation in the prepared solution (0.1% Triton X-100, 0.1% sodium citrate) for 5 min. Cells were then incubated with terminal deoxynucleotidyl transferase dUTP nick end labeling (TUNEL) reaction mixtures in a humidified atmosphere for 1 hr at 37 °C in the dark, washed in PBS, and analyzed by flow cytometry. The BioVision CaspGLOW™ Fluorescein Active Caspase-3 Staining Kit (Milpitas, CA, USA) was used for detection of active caspase 3. For investigating apoptosis in animal cardiac tissues, tissues were soaked in 4% paraformaldehyde. Paraffin-embedded heart was cut into 2-μm-thick sections. TUNEL staining was performed for apoptosis. In brief, the tissue sections were deparaffinized in xylene, rehydrated through a graded alcohol series (100%, 90%, 85%, and 75%), and then rinsed in PBS (pH 7.2). A DNA fragmentation detection kit (FragEL; Calbiochem) was used to detect apoptotic cells in cardiac tissue sections using TUNEL assay.

Investigation of mitochondrial membrane potential

The JC-1 is widely used to study mitochondrial membrane potential. In healthy cells, JC-1 concentrates in the mitochondrial matrix where it forms red fluorescent aggregates. In apoptotic and necrotic cells, JC-1 exists in monomeric form and stains cells green. After stimulation of H/R, cells were rinsed with DMEM and then loaded with JC-1 (5 μM). After 30-min incubation at room temperature, cells were assayed by flow cytometry.

Mitochondrial biogenesis

Real-time polymerase chain reaction (PCR) assay was performed to investigate mitochondrial deoxyribonucleic acid (mtDNA) content. The primers for mitochondrial complex II were sense primer 5’-CAAACCTACGCCAAAATCCA-3’ and antisense primer 5’-GAAATGAATGAGCCTACAGA-3’. The primers forβ-actin were sense primer 5’-AGGTCATCACTATTGGCAACGA-3’ and antisense primer 5’-CACTTCATGATGGAATTGAATGTAGTT-3’. The result of real-time PCR was assayed by SYBR Green on an ABI 7000 sequence detection system according to the protocol.

NADPH oxidase activity assay

The lucigenin method was used to determine the nicotinamide adenine dinucleotide phosphate hydrogen (NADPH) oxidase activity in cells. The crude membrane fraction of cells was prepared by a kit. The total protein concentration was adjusted to 1 mg/mL. An aliquot 200 μL of protein was incubated in the presence of 5 μm lucigenin and 100 μm NADPH. The luminescence was measured after 10 min by a plate reader (VICTOR3; PerkinElmer) to determine the relative changes in NADPH oxidase activity.

Measurement of ROS formation

ROS generation in H9c2 cells was tested using DHE. Cells were pre-treated with or without DAPA for 2 hr. Next, cells were exposed to H/R. After removing the medium from the wells, cells were incubated with 10 μm DHE for 30 min. The fluorescence intensity was calculated by a flow cytometry.

Transfection with small interfering RNA

AMPK siRNA, PGC-1-a siRNA (AMPK ON-TARGET plus SMART pool and PGC-1-a ON-TARGET plus SMART pool) and negative control siRNA (ON-TARGET plus non-targeting pool) were purchased from Dharmacon. Two days after transfection, cells were treated with a reagent as indicated for further experiments.

Statistical analyses

Results are expressed as the means ± standard deviation (SD). Statistical analyses were performed using analysis of variance, followed by Turkey's test. A p value < 0.05 was considered statistically significant.

Results

DAPA stimulates AMPK phosphorylation in H9c2 cells under normoxia and hypoxia/reoxygenation condition

As shown in **Fig.1A and 1B**, the expression of phosphorylated AMPK elevated dose-dependently in cardiac myoblast H9c2 cells following DAPA treatment under normoxia condition. Likewise, the treatment of H9c2 cells with DAPA resulted in a time-dependent increase in the expression of phosphorylated AMPK (**Fig.1C and 1D**). We showed that the activation of AMPK was decreased in response to 1 hr hypoxia with subsequent 4 hr reoxygenation (H1R4) (**Fig.1E-G**), which was consistent with a previous study showing a decline in the level of phosphorylated AMPK was observed after 24 hr of reoxygenation [15]. It has been shown that activation of AMPK was associated with the reduced phosphorylation of protein kinase C (PKC) [16], which was in conformity with our data (**Fig.1E-G**). With the administration of DAPA, the expression of phosphorylated AMPK increased after H1R4, while the phosphorylation of PKC was suppressed in a dose-dependent manner (**Fig.1E-G**). These results suggested that DAPA treatment was able to restore the insufficient AMPK and repress the PKC activation in cardiac myoblast H9c2 cells following H/R condition.

DAPA prevents the hypoxia/reoxygenation-induced oxidative stress through AMPK/ PKC/ NADPH oxidase pathway

NADPH oxidase (Nox) is one of the major sources of ROS production after myocardial reperfusion [17]. The main Nox isoform expressed in cardiomyocytes was Nox-2, which required additional protein subunits, such as Rac1, to become fully activated [18]. Previously, it has been indicated that AMPK may inhibit the generation of ROS via suppression of PKC, which in turn hindered the activation of Nox in a rat model of AMI [16]. As such, we examined whether DAPA attenuated oxidative stress in cardiac myoblast H9c2 cells through inhibition of Nox mediated by the AMPK/PKC pathway. As expected, the expression of Nox-2 and Rac-1 (**Fig. 2A-C**) as well as the Nox activity (**Fig. 2D**) and ROS production (**Fig. 2E**) were all upregulated in H9c2 cells exposed to H/R injury (H1R4). Nevertheless, the H/R-induced Nox-2 and Rac-1 along with the Nox activity and ROS production were abrogated by the treatment of DAPA (**Fig. 2A-E**). We showed that silencing of AMPK abolished the effects of DAPA on suppression of Nox-2 and Rac-1 (**Fig. 2A-C**). Similarly, Nox activity (**Fig. 2D**) and ROS generation (**Fig. 2E**) were reversed in H9c2 cells transfected with si-AMPK. Furthermore, we demonstrated that PKC involved in the H/R-induced Nox activity as administration of Ro-32-0432 (a selective PKC inhibitor) prevented an increase in Nox activity (**Fig. 2D**). Also, we showed that ROS production was mediated by PKC and Nox activation as treatment of Ro-32-0432 and DPI (a Nox inhibitor) both repressed the H/R-stimulated ROS production (**Fig. 2E**). In concert with previous results, our data suggested that DAPA protected H9c2 cells against oxidative stress following H/R injury through modulation of AMPK/ PKC/ Nox signaling.

DAPA reverses the hypoxia/reoxygenation-reduced PGC-1α expression and mitochondrial biogenesis through AMPK/ PKC/ NADPH oxidase pathway

PGC-1α plays a central role in the regulation of the mitochondrial biogenesis and antioxidant gene expression [19] and involves in the AMPK-dependent control of ROS [5]. Here, we showed that the expression of PGC-1α was suppressed following H/R injury whereas treatment of DAPA maintained the amount of PGC-1α (**Fig. 3A and 3B**). Moreover, the silence of AMPK and application of DPI to inhibit Nox both abrogated this effect (**Fig. 3A and 3B**), suggesting that reservation of PGC-1α expression by DAPA was related to oxidative stress inhibition via AMPK activation.

Next, the membrane-permeant JC-1 dye was utilized to measure mitochondrial membrane potential and apoptosis by flow cytometry. We observed a higher percentage of cells expressing JC-1 red fluorescence (FL2) in control cells, while cells subjected to H/R injury displayed the downregulated JC-1 red fluorescence (FL2) and the increased green fluorescence (FL1) **(Fig. 3C and 3D)**. With the administration of DAPA, cells under H/R condition showed a similar red/green fluorescence intensity ratio as control cells, indicating the protective effect of DAPA on the apoptosis caused by H/R injury. Nevertheless, this protective effect was not observed in H/R-injured cells treated with si-AMPK or si-PGC-1α as there were more apoptotic cells expressing green fluorescence (FL1) in these groups. On the other hand, the percentages of FL2/FL1 in cells co-treated with Ro-32-0432 or DPI were comparable to control cells, indicating that PKC and Nox-2 participated in the induction of apoptosis by H/R (**Fig. 3C and 3D)**. As for

mitochondrial DNA copy number, we showed that DAPA limited the H/R-induced dropping of DNA copy number. Likewise, knockdown of AMPK and PGC-1α demonstrated a lower mitochondrial DNA copy number (**Fig. 3E**), indicating upregulation of AMPK and PGC-1α was required for the preservation. Treatment of cells with Ro-32-0432 or DPI showed that repression of PKC and Nox-2 was able to avoid the H/R-reduced mitochondrial DNA copy number.

DAPA diminishes hypoxia/reoxygenation-induced apoptosis and mitigates the activation of caspase-3 via AMPK/ PKC/ NADPH oxidase/ PGC-1α pathway

Aside from the JC-1 assay, we also examined the expression of various apoptosis-related proteins (**Fig. 4A**). The expression level of phosphorylated p53 was upregulated following H/R insult (**Fig. 4B**), and treatment of DAPA dose-dependently downregulated it. We also showed a greater expression of Bax and a less expression of Bcl-2 in cells experienced H/R condition, but DAPA administration seemed to reduce apoptotic susceptibility (**Fig. 4A, 4C, and 4D**). Besides, the expression of cytochrome *c* in each group corresponded with the abovementioned results and showed that DAPA inhibited the H/R-induced cytochrome *c* elevation (**Fig. 4E**). Results from the caspase 3 assessments demonstrated that DAPA impeded the H/R-stimulated caspase 3 activation (**Fig. 4F**). Knockdown of AMPK or PGC-1α in DAPA-treated cells exhibited upregulation of caspase 3 (**Fig. 4F**), indicating that the increase of AMPK or PGC-1α was necessary to the inhibitory effect of DAPA. Application of Ro-32-0432 or DPI showed that downregulation of PKC and Nox-2 repressed the activation of caspase 3. This conclusion was further supported by TUNEL assay (**Fig. 4G**). Taken together, these data demonstrated that DAPA was able to suppress the apoptosis of H9c2 cells in response to H/R insult, which may be mediated by AMPK/ PKC/ Nox/ PGC-1α signaling.

DAPA protects the heart from the damage caused by ischemia/reperfusion injury

We next studied the effect of DAPA on the cardiac function of the AMI rats, which were subjected to 1 hr of LAD occlusion followed by reperfusion for 4 days, representing I/R injuries. Data from echocardiography showed that the ejection fraction (EF) and fractional shortening (FS) were significantly decreased in the heart of I/R injured rats, while administration of DAPA prevented these two values from dropping (**Fig. 5A and 5B**). In addition, the increase of left ventricular end-diastolic and end-systolic volume (LV vol d and LV vol s) as well as the left ventricular internal dimensions at end-diastole and end-systole (LVIDd and LVIDs) were reduced in the I/R injured rats with DAPA treatment compared to those I/R injured rats without DAPA treatment (**Fig. 5C-F**). Representative echocardiographic M-mode images were presented (**Fig. 5G**). These data suggested that DAPA treatment reduced the dilatation and contractile dysfunction of left ventricle caused by I/R injury.

In order to investigate the effect of DAPA on the reduction of apoptosis *in vivo*, we utilized the TUNEL assay to evaluate the apoptosis in the heart of AMI rats. The percentage of TUNEL-positive cells was greater in the I/R injury group compared to the sham group (**Fig. 6A, left and middle panel)** and DAPA treatment significantly reduced the TUNEL-positive cells in I/R injury group **(Fig. 6A, middle and right panel)**, indicating the administration of DAPA ameliorated the I/R-elicited apoptosis in the heart.

Moreover, we showed that the concentration of two enzymes that were used to predict and estimate myocardial injury and infarct size, LDH and CK-MB, were both elevated in the blood following I/R injury (**Fig. 6C and 6D**). Nevertheless, these changes were attenuated in the rats receiving DAPA treatment, which was in agreement with the finding of less myocardial apoptosis. Taken together, these results confirmed that the administration of DAPA ameliorated the myocardial apoptosis and damage following I/R stimulus.

Discussion

Over the past few years, mounting evidence suggested that SGLT2 inhibitors, which were first used as antidiabetic medications, exerted preferentially favorable effects to reduce heart failure and cardiovascular death in DM patients [20, 21]. Among these SGLT2 inhibitors, the benefits of DAPA have been demonstrated in various clinical studies [9–12]. One of the recent *in vivo* experiments even indicated that acute DAPA administration possessed the cardioprotective effects in rats subjected to I/R injury [22]. Several pieces of research have unraveled how DAPA contributes to cardiovascular benefits. First, DAPA may be able to regulate the ionic homeostasis in cardiomyocytes. For instance, DAPA was found to lower the amplitude of the calcium transients in control and type I DM ventricular myocytes [23]. Also, it inhibited the activity of Na^+/H^+ exchanger (NHE) and downregulated cytosolic Na^+ [24], and blockage of NHE has been revealed to reduce ischemic Na^+ overload and enhance the post-ischemic contractile recovery in the heart of rats with I/R injury [25]. Secondly, DAPA reduced the oxidative stress and prolonged ventricular repolarization via augmentation of mitochondrial function. It has been shown to preserve the depolarized mitochondrial membrane potential, and enhance cytosolic calcium homeostasis [26]. In line with these findings, we showed that the administration of DAPA suppressed the production of ROS. Besides, it reversed the altered mitochondrial membrane potential and DNA copy number following H/R insult, which attenuated the subsequent apoptosis. Most importantly, our data further elucidated that AMPK activation played a significant role in the DAPA-regulated mitochondrial energetics (Fig. 7).

As an energy sensor, AMPK orchestrated multiple metabolic responses to energy deprivation, and modulation of AMPK has been thought to be the key to the prevention of reinfarction or apoptosis. Certainly, numerous clinically approved medications that upregulated AMPK, such as metformin [27] and aspirin [28, 29], have been shown to hold the potential to ameliorate myocardial I/R injury. Here, we provided the evidence to substantiate that AMPK phosphorylation by DAPA activated PGC-1α, the crucial modulator of mitochondrial function and oxidative metabolism in the heart. Previously, AMPK has been shown to directly phosphorylate PGC-1α at threonine-177 and serine-538 in the skeletal muscle [30], and our results suggested that the DAPA-induced AMPK upregulated PGC-1α via PKC/Nox pathway. PGC-1α deficiency has been proven to diminish normal cardiac function [31], and it has been shown that AMPK/PGC-1α axis participated in the acetylcholine-induced [32] and metformin-associated [33] cardioprotective effects. In the present study, we showed that the restoration of PGC-1α by DAPA reduced the mitochondrial dysfunction and myocardial apoptosis following H/R insult, which was consistent with

various studies showing PGC-1α mediated mitochondrial oxidative damage and apoptotic susceptibility [34, 35].

Besides, AMPK activation has been known to suppress oxidative stress via multiple mechanisms. For instance, AMPK activation eliminated the hyperglycemia-induced mitochondrial ROS through elevation of manganese superoxide dismutase and enhancement of mitochondrial biogenesis in human umbilical vein endothelial cells (HUVECs) [36]. Additionally, AMPK phosphorylation increased the expression of mitochondrial uncoupling protein-2, leading to the inhibition of both superoxide anions and prostacyclin synthase nitration in HUVECs [37]. AMPK was also implicated in the regulation of Nox pathway, which was indispensable for the accumulation of oxidative stress following myocardial I/R injury [38]. Various studies have suggested that AMPK activation mitigated glucose-induced oxidative stress through Nox suppression [39, 40]. Loss of AMPK activity has been reported to elevate the expression of several Nox subunits and the oxidase-mediated superoxide production in endothelial cells [41]. Moreover, it has been demonstrated that AMPK phosphorylation by rosiglitazone may inhibit PKC, which impeded the Nox activation and glucose-induced oxidative stress in HUVECs [39]. Another study showed a similar finding that AMPK may hamper the PKC-mediated accumulation of ROS by suppression of Nox [16]. Likewise, we showed that the upregulation of AMPK was associated with the repression of PKC, leading to a diminution in Nox-2 activity in cells treated with DAPA. Among various Nox isoforms, Nox-1 and Nox-2 have been demonstrated to mediate myocardial oxidative damage during reperfusion, and Nox-2 also participated in the generation of oxidative stress post-reperfusion [38]. Our results disclosed that administration of DAPA reduced the Nox-2-mediated oxidative stress. Further investigation of whether DAPA attenuates organ damage and displays Nox-2 suppressive effect in other I/R injury models may represent an intriguing subject.

Apart from the *in vitro* experiment, we examined the effects of DAPA on cardiac function and myocardial apoptosis. Data from echocardiography revealed that DAPA administration improved the measurement of LV function (such as EF and FS) affected by I/R injury, and this was in line with a recent study revealing the positive effect of DAPA on the enhancement of LV function of Type II DM patients with stable heart failure [9]. Moreover, we showed that treatment of DAPA attenuated the rise in the levels of two AMI-associated enzymes (CK-MB and LDH) in response to I/R injury, which was in conformity with a study showing SGLT2 inhibitor exhibited cardioprotective effects and downregulated the serum CK-MB and LDH in DM rats [42]. Taken together, DAPA may have protective effect of cardiac function in the setting of AMI.

Conclusions

Overall, the current study demonstrated that DAPA reduced the extent of myocardial injury and apoptosis and improved cardiac contractile function in the I/R injured heart. Our data revealed that AMPK/ PKC/ Nox/ PGC-1α signaling mediated the cardioprotection of DAPA against I/R injury and provided molecular insight into the probable benefit of DAPA for patients with AMI.

Declarations

Authors' contributions K-L T, P-L H and S-H C conceived and designed this study. W-C C and H-C C collected the data. K-L T, W-C C, H-C C and Y-T H performed this study. P-L H, Y-T H and S-H C contributed analysis tools. K-L T, P-L H and S-H C wrote this paper.

Acknowledgments None.

Funding This study was supported by Ministry of Science and Technology, Taiwan (MOST-108-2320-B-006 -053) and National Cheng Kung University Hospital, Taiwan (NCKUH-10902010).

Declaration of competing interest None.

Consent for publication Not applicable.

Availability of data and materials All data are provided in this paper.

Ethics approval and consent to participate This study was approved by the IACUC committees at National Cheng Kung University.

Abbreviations

Dapagliflozin (DAPA), ischemia/reperfusion (I/R), adenosine 5'-monophosphate activated protein kinase (AMPK), phosphorylated protein kinase C (PKC), hypoxia/reoxygenation (H/R), peroxisome proliferator-activated receptor-gamma coactivator 1-alpha (PGC-1α), cardiovascular diseases (CVD), acute myocardial infarction (AMI), adenosine triphosphate (ATP), sodium-glucose transporter 2 (SGLT2), diabetes mellitus (DM), Dulbecco's modified Eagle's medium (DMEM), fetal bovine serum (FBS), ethylenediaminetetraacetic acid (EDTA), 5,58,6,68-tetraethylbenzimidazolcarbocyanine iodide (JC-1), Dihydroethidium (DHE), Horseradish peroxidase (HRP), radioimmunoprecipitation assay (RIPA), polyvinylidene difluoride (PVDF), lactate dehydrogenase (LDH), terminal deoxynucleotidyl transferase dUTP nick end labeling (TUNEL), nicotinamide adenine dinucleotide phosphate hydrogen (NADPH), ejection fraction (EF), fractional shortening (FS), left ventricular end-diastolic volume (LV vol d), left ventricular end-systolic volume (LV vol s), left ventricular internal dimensionse (LVIDd) at end-diastole and end-systole (LVIDs).

References

1. Mozaffarian D, Benjamin EJ, Go AS, Arnett DK, Blaha MJ, Cushman M, de Ferranti S, Després JP, Fullerton HJ, Howard VJ, et al. Heart disease and stroke statistics–2015 update: a report from the American Heart Association. Circulation. 2015;131(4):e29–322.
2. Fournier JA, Cabezón S, Cayuela A, Ballesteros SM, Cortacero JA, Díaz De La Llera LS. Long-term prognosis of patients having acute myocardial infarction when </=40 years of age. The American journal of cardiology. 2004;94(8):989–92.

3. O'Gara PT, Kushner FG, Ascheim DD, Casey DE Jr, Chung MK, de Lemos JA, Ettinger SM, Fang JC, Fesmire FM, Franklin BA, et al. 2013 ACCF/AHA guideline for the management of ST-elevation myocardial infarction: a report of the American College of Cardiology Foundation/American Heart Association Task Force on Practice Guidelines. J Am Coll Cardiol. 2013;61(4):e78–140.
4. Kalogeris T, Bao Y, Korthuis RJ. Mitochondrial reactive oxygen species: a double edged sword in ischemia/reperfusion vs preconditioning. Redox Biol. 2014;2:702–14.
5. Rabinovitch RC, Samborska B, Faubert B, Ma EH, Gravel SP, Andrzejewski S, Raissi TC, Pause A, St-Pierre J, Jones RG. AMPK Maintains Cellular Metabolic Homeostasis through Regulation of Mitochondrial Reactive Oxygen Species. Cell Rep. 2017;21(1):1–9.
6. Russell RR 3rd, Li J, Coven DL, Pypaert M, Zechner C, Palmeri M, Giordano FJ, Mu J, Birnbaum MJ, Young LH. AMP-activated protein kinase mediates ischemic glucose uptake and prevents postischemic cardiac dysfunction, apoptosis, and injury. J Clin Invest. 2004;114(4):495–503.
7. Kim AS, Miller EJ, Wright TM, Li J, Qi D, Atsina K, Zaha V, Sakamoto K, Young LH. A small molecule AMPK activator protects the heart against ischemia-reperfusion injury. J Mol Cell Cardiol. 2011;51(1):24–32.
8. Thomas MC, Cherney DZI. The actions of SGLT2 inhibitors on metabolism, renal function and blood pressure. Diabetologia. 2018;61(10):2098–107.
9. Tanaka H, Soga F, Tatsumi K, Mochizuki Y, Sano H, Toki H, Matsumoto K, Shite J, Takaoka H, Doi T, et al. Positive effect of dapagliflozin on left ventricular longitudinal function for type 2 diabetic mellitus patients with chronic heart failure. Cardiovasc Diabetol. 2020;19(1):6.
10. Kato ET, Silverman MG, Mosenzon O, Zelniker TA, Cahn A, Furtado RHM, Kuder J, Murphy SA, Bhatt DL, Leiter LA, et al. Effect of Dapagliflozin on Heart Failure and Mortality in Type 2 Diabetes Mellitus. Circulation. 2019;139(22):2528–36.
11. Wiviott SD, Raz I, Bonaca MP, Mosenzon O, Kato ET, Cahn A, Silverman MG, Zelniker TA, Kuder JF, Murphy SA, et al. Dapagliflozin and Cardiovascular Outcomes in Type 2 Diabetes. N Engl J Med. 2019;380(4):347–57.
12. Furtado RHM, Bonaca MP, Raz I, Zelniker TA, Mosenzon O, Cahn A, Kuder J, Murphy SA, Bhatt DL, Leiter LA, et al. Dapagliflozin and Cardiovascular Outcomes in Patients With Type 2 Diabetes Mellitus and Previous Myocardial Infarction. Circulation. 2019;139(22):2516–27.
13. Han Y, Cho YE, Ayon R, Guo R, Youssef KD, Pan M, Dai A, Yuan JX, Makino A. SGLT inhibitors attenuate NO-dependent vascular relaxation in the pulmonary artery but not in the coronary artery. Am J Physiol Lung Cell Mol Physiol. 2015;309(9):L1027–36.
14. Ye Y, Bajaj M, Yang HC, Perez-Polo JR, Birnbaum Y. SGLT-2 Inhibition with Dapagliflozin Reduces the Activation of the Nlrp3/ASC Inflammasome and Attenuates the Development of Diabetic Cardiomyopathy in Mice with Type 2 Diabetes. Further Augmentation of the Effects with Saxagliptin, a DPP4 Inhibitor. Cardiovasc Drugs Ther. 2017;31(2):119–32.
15. Kuznetsov AV, Javadov S, Sickinger S, Frotschnig S, Grimm M. H9c2 and HL-1 cells demonstrate distinct features of energy metabolism, mitochondrial function and sensitivity to hypoxia-

reoxygenation. Biochim Biophys Acta. 2015;1853(2):276–84.

16. Kong SS, Liu JJ, Yu XJ, Lu Y, Zang WJ. Protection against ischemia-induced oxidative stress conferred by vagal stimulation in the rat heart: involvement of the AMPK-PKC pathway. Int J Mol Sci. 2012;13(11):14311–25.
17. Yellon DM, Hausenloy DJ. Myocardial reperfusion injury. N Engl J Med. 2007;357(11):1121–35.
18. Akki A, Zhang M, Murdoch C, Brewer A, Shah AM. NADPH oxidase signaling and cardiac myocyte function. J Mol Cell Cardiol. 2009;47(1):15–22.
19. St-Pierre J, Drori S, Uldry M, Silvaggi JM, Rhee J, Jäger S, Handschin C, Zheng K, Lin J, Yang W, et al. Suppression of reactive oxygen species and neurodegeneration by the PGC-1 transcriptional coactivators. Cell. 2006;127(2):397–408.
20. Kaplan A, Abidi E, El-Yazbi A, Eid A, Booz GW, Zouein FA. Direct cardiovascular impact of SGLT2 inhibitors: mechanisms and effects. Heart Fail Rev. 2018;23(3):419–37.
21. Uthman L, Baartscheer A, Schumacher CA, Fiolet JWT, Kuschma MC, Hollmann MW, Coronel R, Weber NC, Zuurbier CJ. Direct Cardiac Actions of Sodium Glucose Cotransporter 2 Inhibitors Target Pathogenic Mechanisms Underlying Heart Failure in Diabetic Patients. Front Physiol. 2018;9:1575.
22. Lahnwong S, Palee S, Apaijai N, Sriwichaiin S, Kerdphoo S, Jaiwongkam T, Chattipakorn SC, Chattipakorn N. Acute dapagliflozin administration exerts cardioprotective effects in rats with cardiac ischemia/reperfusion injury. Cardiovasc Diabetol. 2020;19(1):91.
23. Hamouda NN, Sydorenko V, Qureshi MA, Alkaabi JM, Oz M, Howarth FC. Dapagliflozin reduces the amplitude of shortening and Ca(2+) transient in ventricular myocytes from streptozotocin-induced diabetic rats. Mol Cell Biochem. 2015;400(1–2):57–68.
24. Uthman L, Baartscheer A, Bleijlevens B, Schumacher CA, Fiolet JWT, Koeman A, Jancev M, Hollmann MW, Weber NC, Coronel R, et al. Class effects of SGLT2 inhibitors in mouse cardiomyocytes and hearts: inhibition of Na(+)/H(+) exchanger, lowering of cytosolic Na(+) and vasodilation. Diabetologia. 2018;61(3):722–6.
25. ten Hove M, van Emous JG, van Echteld CJ. Na + overload during ischemia and reperfusion in rat hearts: comparison of the Na+/H + exchange blockers EIPA, cariporide and eniporide. Mol Cell Biochem. 2003;250(1–2):47–54.
26. Durak A, Olgar Y, Degirmenci S, Akkus E, Tuncay E, Turan B. A SGLT2 inhibitor dapagliflozin suppresses prolonged ventricular-repolarization through augmentation of mitochondrial function in insulin-resistant metabolic syndrome rats. Cardiovasc Diabetol. 2018;17(1):144.
27. Higgins L, Palee S, Chattipakorn SC, Chattipakorn N. Effects of metformin on the heart with ischaemia-reperfusion injury: Evidence of its benefits from in vitro, in vivo and clinical reports. Eur J Pharmacol. 2019;858:172489.
28. Frilling B, Schiele R, Gitt AK, Zahn R, Schneider S, Glunz HG, Gieseler U, Jagodzinski E, Senges J. Too little aspirin for secondary prevention after acute myocardial infarction in patients at high risk for cardiovascular events: Results from the MITRA study. Am Heart J. 2004;148(2):306–11.

29. Verheugt FW, van der Laarse A, Funke-Küpper AJ, Sterkman LG, Galema TW, Roos JP. Effects of early intervention with low-dose aspirin (100 mg) on infarct size, reinfarction and mortality in anterior wall acute myocardial infarction. The American journal of cardiology. 1990;66(3):267–70.
30. Jäger S, Handschin C, St-Pierre J, Spiegelman BM. AMP-activated protein kinase (AMPK) action in skeletal muscle via direct phosphorylation of PGC-1alpha. Proc Natl Acad Sci U S A. 2007;104(29):12017–22.
31. Leone TC, Lehman JJ, Finck BN, Schaeffer PJ, Wende AR, Boudina S, Courtois M, Wozniak DF, Sambandam N, Bernal-Mizrachi C, et al. PGC-1alpha deficiency causes multi-system energy metabolic derangements: muscle dysfunction, abnormal weight control and hepatic steatosis. PLoS Biol. 2005;3(4):e101.
32. Sun L, Zhao M, Yu XJ, Wang H, He X, Liu JK, Zang WJ. Cardioprotection by acetylcholine: a novel mechanism via mitochondrial biogenesis and function involving the PGC-1α pathway. J Cell Physiol. 2013;228(6):1238–48.
33. Whittington HJ, Hall AR, McLaughlin CP, Hausenloy DJ, Yellon DM, Mocanu MM. Chronic metformin associated cardioprotection against infarction: not just a glucose lowering phenomenon. Cardiovasc Drugs Ther. 2013;27(1):5–16.
34. Villeneuve C, Guilbeau-Frugier C, Sicard P, Lairez O, Ordener C, Duparc T, De Paulis D, Couderc B, Spreux-Varoquaux O, Tortosa F, et al: p53-PGC-1α pathway mediates oxidative mitochondrial damage and cardiomyocyte necrosis induced by monoamine oxidase-A upregulation: role in chronic left ventricular dysfunction in mice. *Antioxid Redox Signal* 2013, 18(1):5–18.
35. Adhihetty PJ, Uguccioni G, Leick L, Hidalgo J, Pilegaard H, Hood DA. The role of PGC-1alpha on mitochondrial function and apoptotic susceptibility in muscle. Am J Physiol Cell Physiol. 2009;297(1):C217–25.
36. Kukidome D, Nishikawa T, Sonoda K, Imoto K, Fujisawa K, Yano M, Motoshima H, Taguchi T, Matsumura T, Araki E. Activation of AMP-activated protein kinase reduces hyperglycemia-induced mitochondrial reactive oxygen species production and promotes mitochondrial biogenesis in human umbilical vein endothelial cells. Diabetes. 2006;55(1):120–7.
37. Xie Z, Zhang J, Wu J, Viollet B, Zou MH. Upregulation of mitochondrial uncoupling protein-2 by the AMP-activated protein kinase in endothelial cells attenuates oxidative stress in diabetes. Diabetes. 2008;57(12):3222–30.
38. Braunersreuther V, Montecucco F, Asrih M, Pelli G, Galan K, Frias M, Burger F, Quinderé AL, Montessuit C, Krause KH, et al. Role of NADPH oxidase isoforms NOX1, NOX2 and NOX4 in myocardial ischemia/reperfusion injury. J Mol Cell Cardiol. 2013;64:99–107.
39. Ceolotto G, Gallo A, Papparella I, Franco L, Murphy E, Iori E, Pagnin E, Fadini GP, Albiero M, Semplicini A, et al. Rosiglitazone reduces glucose-induced oxidative stress mediated by NAD(P)H oxidase via AMPK-dependent mechanism. Arterioscler Thromb Vasc Biol. 2007;27(12):2627–33.
40. Balteau M, Van Steenbergen A, Timmermans AD, Dessy C, Behets-Wydemans G, Tajeddine N, Castanares-Zapatero D, Gilon P, Vanoverschelde JL, Horman S, et al. AMPK activation by glucagon-

like peptide-1 prevents NADPH oxidase activation induced by hyperglycemia in adult cardiomyocytes. Am J Physiol Heart Circ Physiol. 2014;307(8):H1120–33.

41. Wang S, Zhang M, Liang B, Xu J, Xie Z, Liu C, Viollet B, Yan D, Zou MH. AMPKalpha2 deletion causes aberrant expression and activation of NAD(P)H oxidase and consequent endothelial dysfunction in vivo: role of 26S proteasomes. Circ Res. 2010;106(6):1117–28.
42. Hussein AM, Eid EA, Taha M, Elshazli RM, Bedir RF, Lashin LS. Comparative Study of the Effects of GLP1 Analog and SGLT2 Inhibitor against Diabetic Cardiomyopathy in Type 2 Diabetic Rats: Possible Underlying Mechanisms. *Biomedicines* 2020, 8(3).

Figures

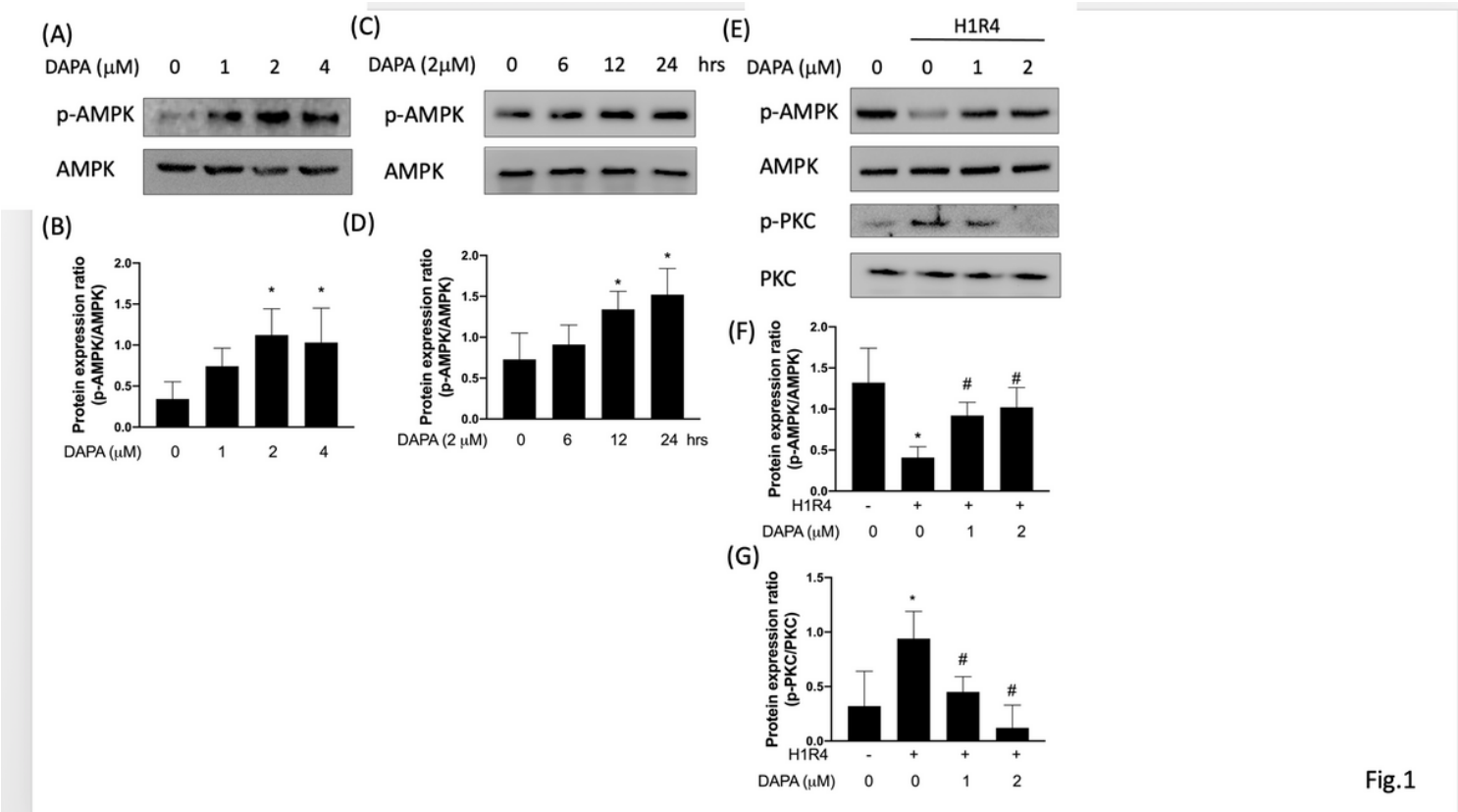

Figure 1

Administration of Dapagliflozin (DAPA) increases the phosphorylation of AMPK and suppresses the phosphorylation of PKC under hypoxia/reoxygenation condition The expression levels of phosphorylated AMPK in H9c2 cells treated with DAPA were enhanced in dose-dependent (A and B) and time-dependent (C and D) manners. Representative Western blot images (E) and relative densitometric bar graphs of phosphorylated-AMPK/AMPK (F) and phosphorylated-PKC/PKC (G) in H9c2 cells exposed to hypoxia for 1 hr and reoxygenation for 4 hr (H1R4) were shown. The data were presented as the means ± SD of three independent experiments (* indicating $p < 0.05$ compared with the control group; # indicating $p < 0.05$ compared to H1R4 condition without DAPA treatment).

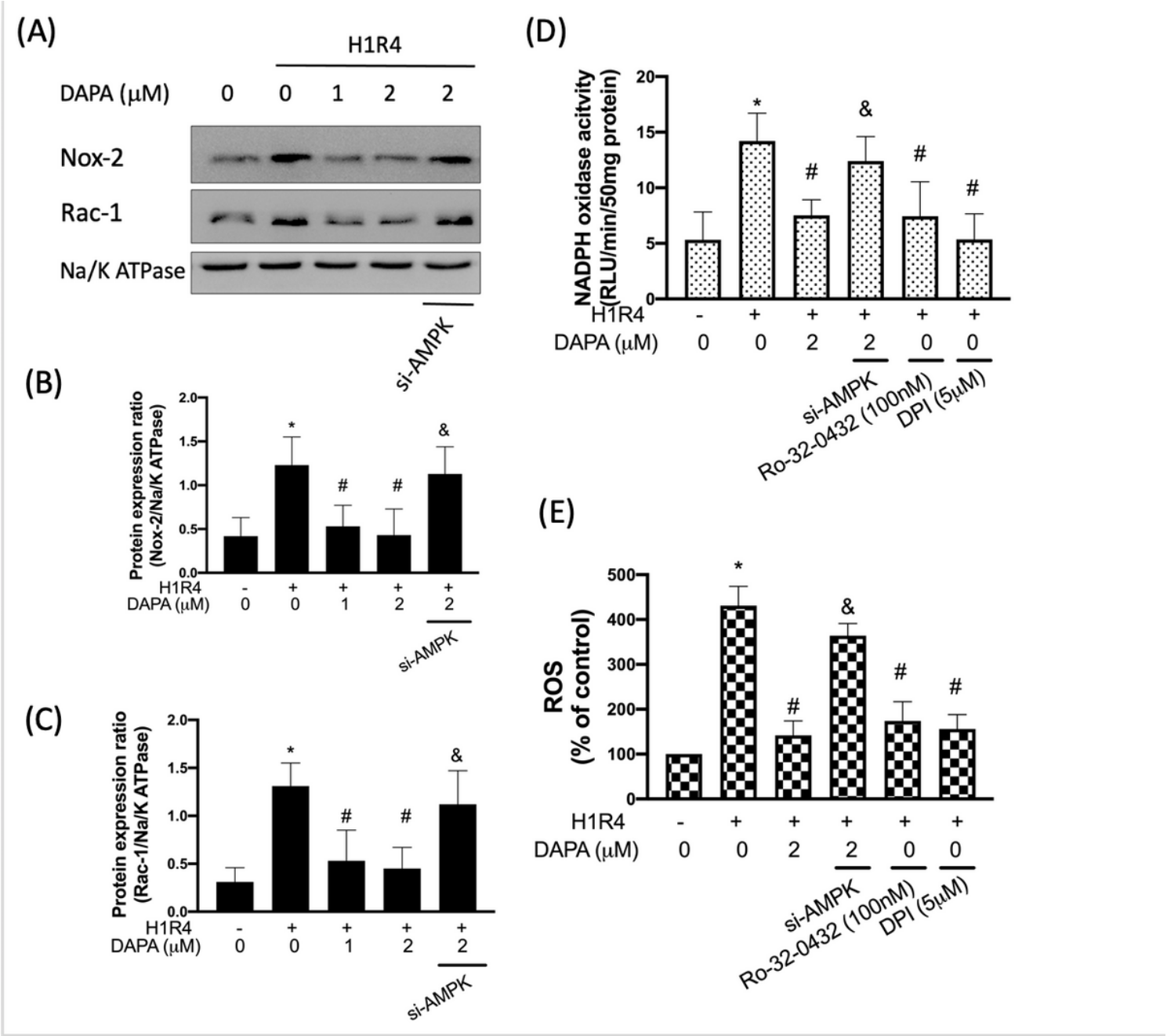

Figure 2

Dapagliflozin (DAPA) prevents the upregulation of ROS via AMPK/ PKC/ NADPH oxidase signaling Representative Western blot images (A) and relative densitometric bar graphs of Nox-2/Na/K ATPase (B) and Rac-1/Na/K ATPase (C) in H9c2 cells exposed to hypoxia for 1 hr and reoxygenation for 4 hr (H1R4) were shown. Activity of NADPH oxidase was measured (D). ROS generation was measured using a flow cytometry to examine the fluorescent intensity of cells (E). The data were presented as the means ± SD of three independent experiments (* indicating $p < 0.05$ compared with the control group; # indicating $p < 0.05$ compared to H1R4 condition without DAPA treatment; & indicating $p < 0.05$ compared with the DAPA-treated cells in H1R4 condition).

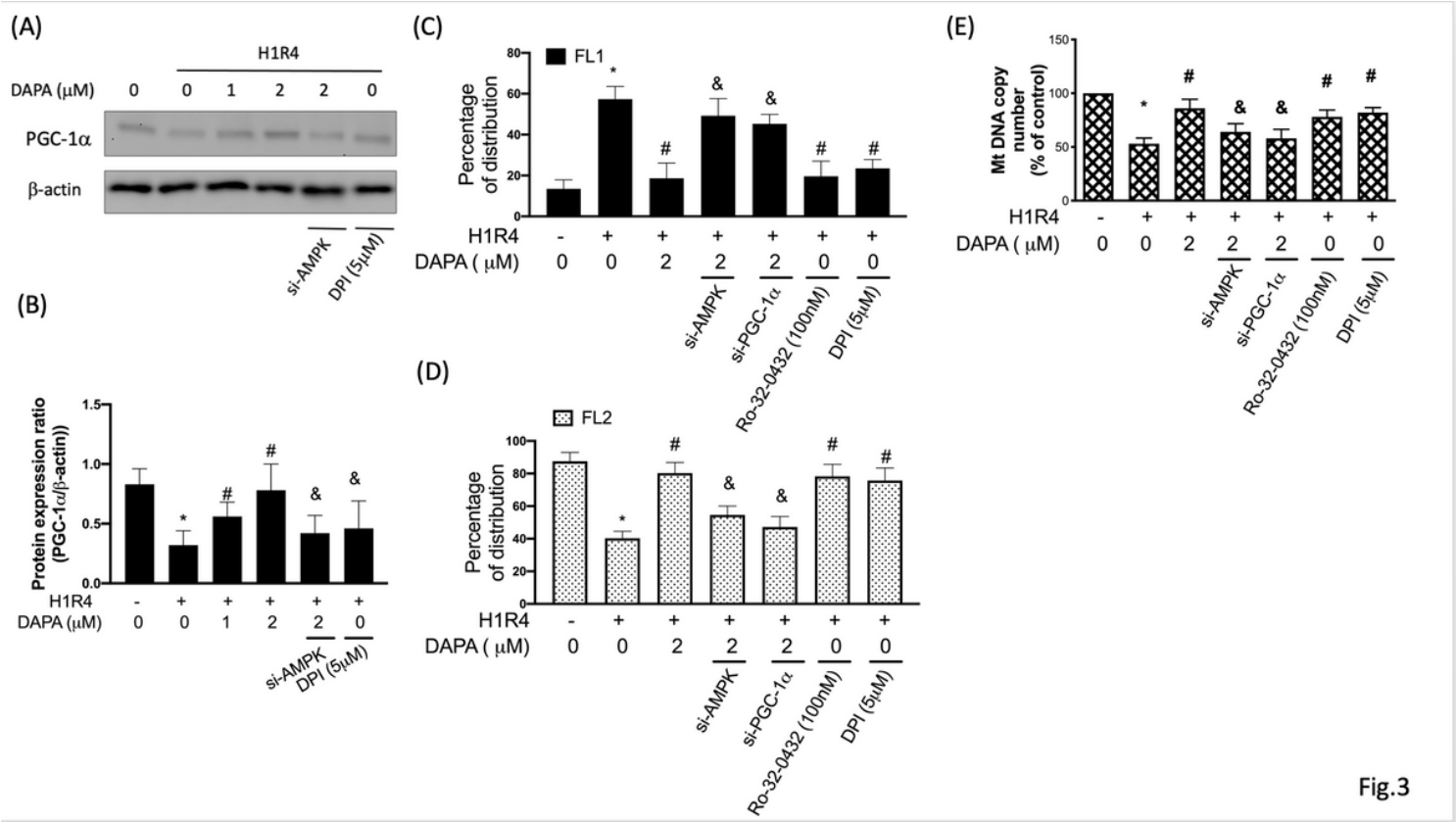

Figure 3

Dapagliflozin (DAPA) prevents hypoxia/reoxygenation-induced PGC-1α downregulation and dysfunction of mitochondrial biogenesis Representative Western blot images (A) and relative densitometric bar graphs (B) of PGC-1α/β-actin in H9c2 cells exposed to hypoxia for 1 hr and reoxygenation for 4 hr (H1R4) were shown. In some cases, cells were transfected with AMPK siRNA 48 hr or pretreated with DPI before exposure to hypoxia/reoxygenation. Percentage of cells expressing JC-1 monomers (green fluorescence; FL1) (C) and JC-1 aggregates (red fluorescence; FL2) (D) were assessed using flow cytometry. (E) Mitochondrial DNA copy numbers were examined after stimulation of hypoxia/reoxygenation. The data were presented as the means ± SD of three independent experiments (* indicating $p < 0.05$ compared with the control group; # indicating $p < 0.05$ compared to H1R4 condition without DAPA treatment; & indicating $p < 0.05$ compared with the DAPA-treated cells in H1R4 condition).

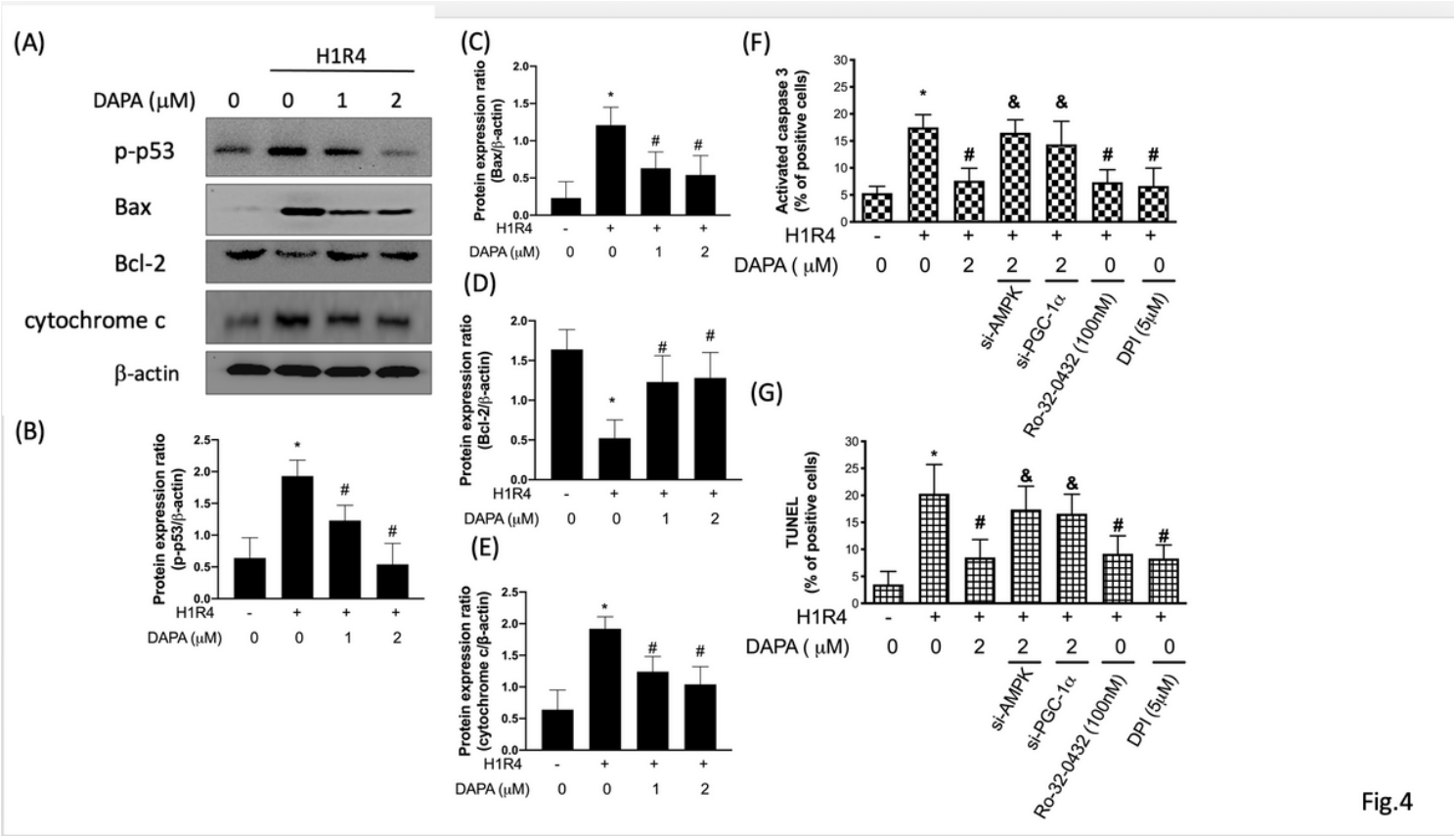

Fig.4

Figure 4

Dapagliflozin (DAPA) prevents hypoxia/reoxygenation-induced apoptosis through AMPK-modulated mitochondrial-dependent pathway Representative Western blot images (A) and relative densitometric bar graphs (B-E) of mitochondrial-dependent apoptotic markers H9c2 cells exposed to hypoxia for 1 hr and reoxygenation for 4 hr (H1R4) were shown. Antiapoptotic effect of DAPA was further confirmed by caspase 3 activity (F) and TUNEL assay (G). The data were presented as the means ± SD of three independent experiments (* indicating $p < 0.05$ compared with the control group; # indicting $p < 0.05$ compared to H1R4 condition without DAPA treatment; & indicating $p < 0.05$ compared the DAPA-treated cells in H1R4 condition).

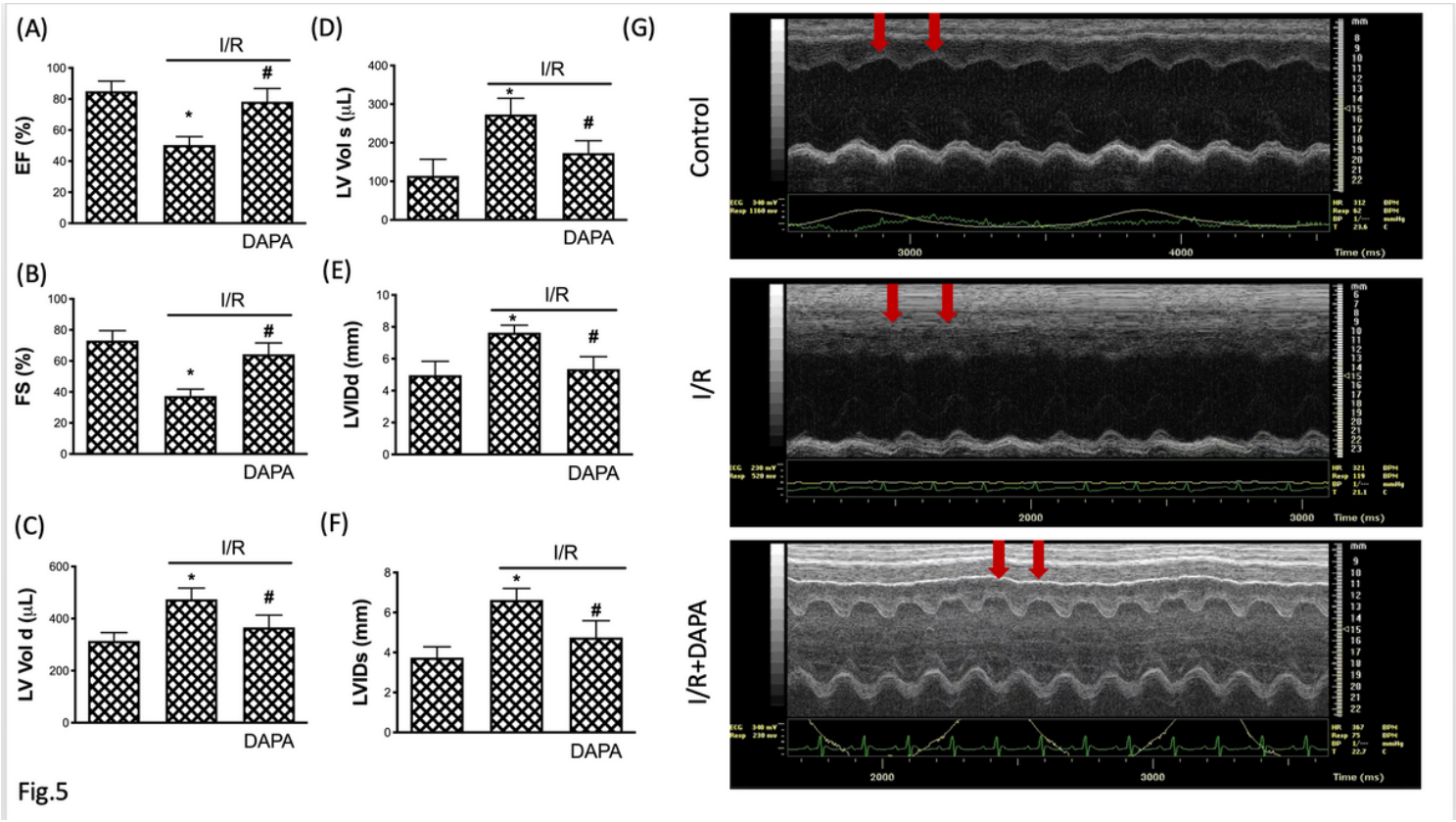

Figure 5

Dapagliflozin (DAPA) protects heart function on ischemia/reperfusion injury Measurement in echocardiography, including (A) ejection fraction, (B) fractional shortening, (C) left ventricular end-diastolic volume, (D) left ventricular end-systolic volume, (E) left ventricular internal dimension at end-diastole, and (F) left ventricular internal dimension at end-systole, were shown. (G) Representative echocardiographic M-mode images from animals in different conditions revealed reduced motion of anterior wall of left ventricle caused by ischemia/reperfusion (I/R) (middle panel), which was attenuated by DAPA treatment (lower panel). Red arrows indicate the motion of anterior wall of left ventricle. The data were presented as the means ± SD of three independent experiments (* indicating $p < 0.05$ compared with the control group; # indicating $p < 0.05$ compared to I/R without DAPA treatment).

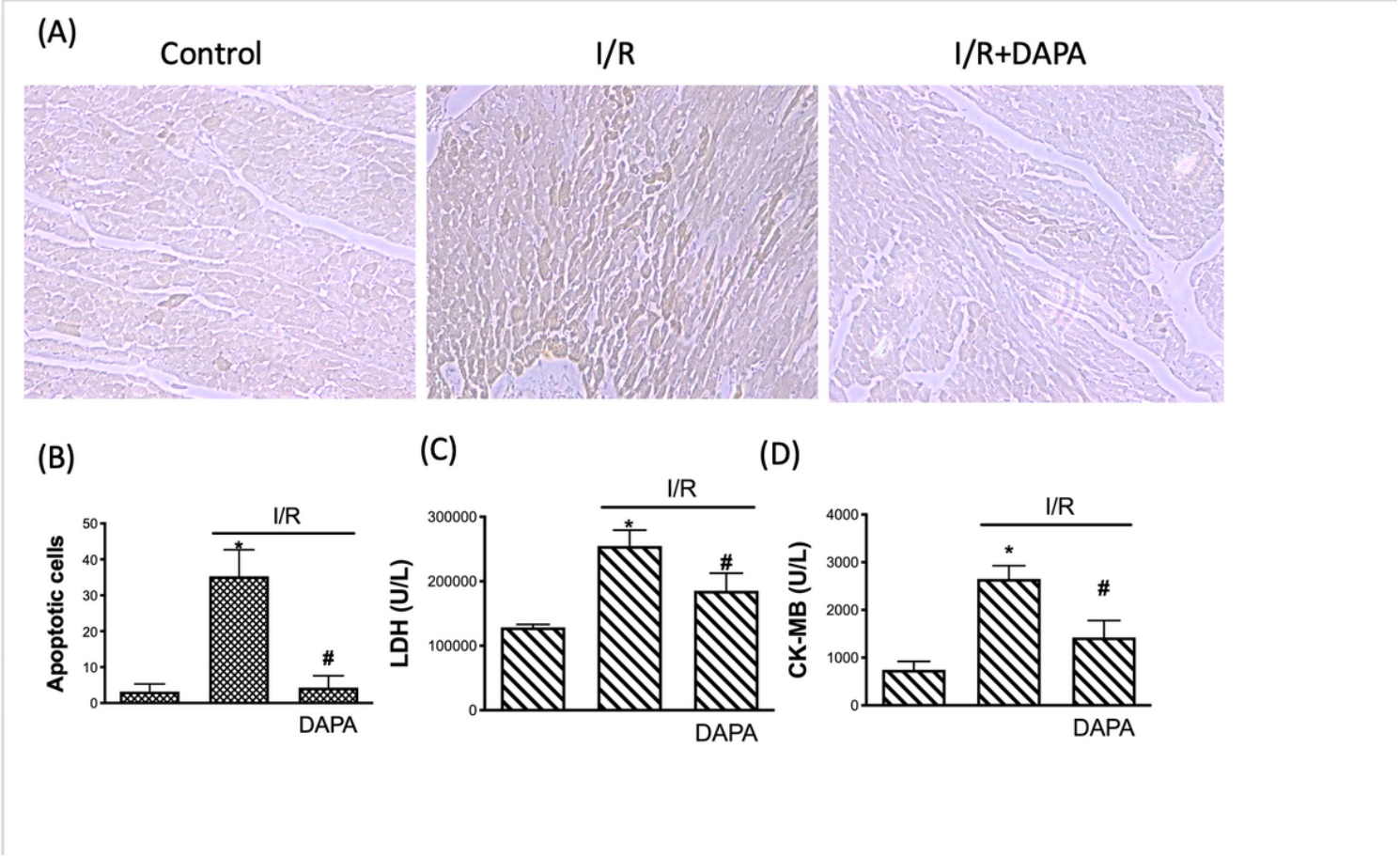

Figure 6

Anti-apoptotic effect of Dapagliflozin (DAPA) on ischemia/reperfusion injured animals Representative image of TUNEL staining of the cardiac tissues (A) and quantification of the apoptotic areas (B) were shown. The plasma concentration of myocardial damage markers, lactate dehydrogenase (LDH) (C) and creatine kinase-MB (CK-MB) (D), in ischemia/reperfusion (I/R) animals with or without DAPA treatment were checked. The data were presented as the means ± SD of three independent experiments (* indicating $p < 0.05$ compared with the control group; # indicating $p < 0.05$ compared to ischemia/reperfusion without DAPA treatment).

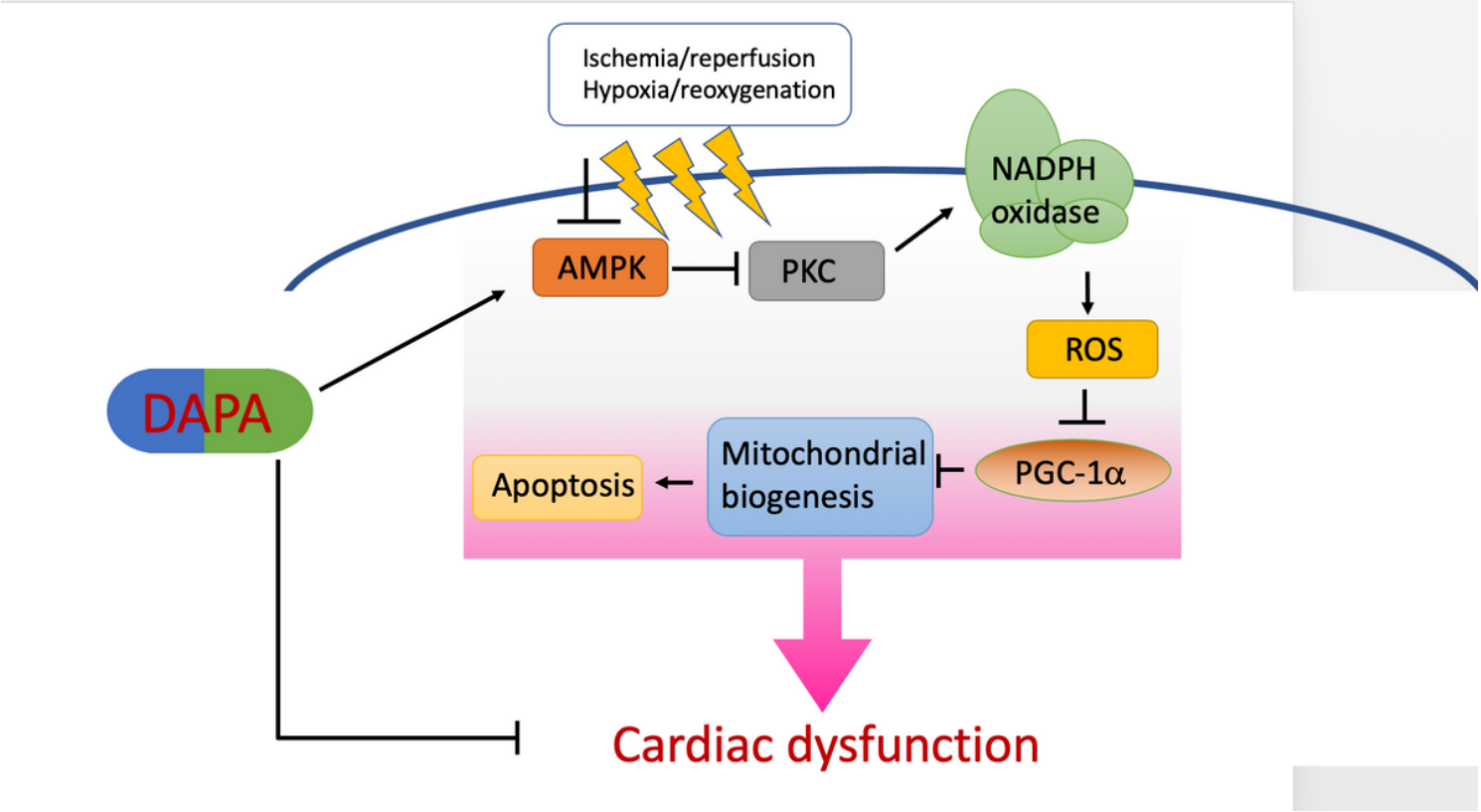

Figure 7

Schematic diagram showing protective signaling of Dapagliflozin (DAPA) on ischemia/reperfusion-caused cardiac dysfunction